# Oxygen-vacancy ordering in the $Ba_2YCu_3O_{7-x}$ $(0 \leq x \leq 1)$ superconducting system

C. Chaillout, M. A. Alario-Franco,* J. J. Capponi, J. Chenavas, J. L. Hodeau, and M. Marezio†
*Laboratoire de Cristallographie, 166X, 38042, Grenoble Cedex, France*
(Received 10 July 1987)

Diffuse scattering streaks or bands have been observed in electron diffraction photographs for samples belonging to the superconducting system $Ba_2YCu_3O_{7-x}$ $(0 \leq x \leq 1)$. *In situ* experiments show that this diffuse scattering can be associated with short-range ordering of oxygen vacancies. The same vacancy ordering occurs in previously reduced samples. Three types of diffuse scattering are observed, each corresponding to a short-range-order scheme.

Many studies on the high-$T_c$ superconductor, $Ba_2YCu_3O_{7-x}$, have shown the great influence of the oxygen composition on the physical properties of these compounds and especially on the superconducting transition temperature.[1,2] This influence is related to the presence of oxygen vacancies which modify the coordination polyhedra around the copper cations. These variations of composition depend on the preparation conditions and the subsequent heat treatments of the samples.

Concerning the $Ba_2YCu_3O_{7-x}$ oxide family, the structure of the end member $Ba_2YCu_3O_7$,[3-6] and of a reduced compound $Ba_2YCu_3O_{6.8}$ (Ref. 5) were recently determined by powder neutron diffraction, and that of $Ba_{2.1}Y_{0.9}Cu_3O_6$ was determined by single-crystal x-ray diffraction.[7] It has also been shown[1,8] that when heated above 500 °C in air, $Ba_2YCu_3O_{7-x}$ can reversibly lose oxygen, in the range of $0 \leq x \leq 1$. As the oxygen composition changes as a function of temperature, at about 650 °C, the symmetry transforms from orthorhombic to tetragonal. We studied, using electron diffraction, several $Ba_2YCu_3O_{7-x}$ samples having different average oxygen compositions, in order to establish how the oxygen deficiency was accommodated in the structure.

The stoichiometric $Ba_2YCu_3O_7$ sample was annealed in oxygen according to a process described in Ref. 3. Three different methods were used to obtain oxygen-deficient samples $(x > 0)$:

(a) By quenching in air from 950 °C. The samples, shaped as small pellets of average size 0.5×0.5×0.5 cm were quickly removed from the furnace and transfered into a thick-walled cold silica crucible. This resulted in rapid cooling, but the samples obtained were not completely homogeneous.

(b) By quenching in liquid nitrogen from 950 °C. This procedure gave more homogeneous, tetragonal-symmetry samples than those obtained by quenching in air. According to the oxygen composition versus temperature curve of Ref. 8, the average composition of this sample is $Ba_2YCu_3O_{6.25}$.

(c) By slow cooling in argon atmosphere from a given temperature corresponding to a given oxygen composition according to Ref. 8, three samples of respective composition $Ba_2YCu_3O_{6.63}$, $Ba_2YCu_3O_{6.41}$, $Ba_2YCu_3O_{6.10}$ were obtained.

Electron-diffraction patterns (Philips EM 400 T, 120 kV) were obtained on the same samples as those studied by powder neutron diffraction.[3,9] In most samples we did not see any splitting of the $c^*$ axis on diffraction patterns along the [100] zone axis (Fig. 1) and no planar defects in images such as those reported in Refs. 10–13. Our observations agree with high-resolution electron microscopy experiments[14] performed on the same sample. Furthermore, neutron-diffraction refinements did not show any Y/Ba substitution.

We studied the ordered samples having different oxygen compositions. The majority of electron-diffraction patterns corresponding to reduced samples $(x > 0)$ obtained by quenching in air show diffuse scattering as well as Bragg reflexions. Three different kinds of diffuse scattering have been observed depending on the sample.

In the first case, diffuse lines parallel to the $c^*$ axis are present on diffraction patterns corresponding to the principal Laüe zones. Their intersection with the $(001)^*$ reciprocal plane can be indexed as (000), $(\frac{1}{2}00)$, $(0\frac{1}{2}0)$, $(\frac{1}{2}\frac{1}{2}0)$, (100), (010), $(\frac{3}{4}\frac{1}{4}0)$, etc. Figures 2(a)–2(d) show diffraction patterns along, respectively, $[0\bar{1}0]$, $[1\bar{1}0]$, $[1\bar{2}0]$, and $[1\bar{3}0]$ zone axes, and one can clearly see these diffuse lines. They are sharp in the $a^*b^*$ plane and continuous along $c^*$ direction. The intensity of those located between principal zones is modulated along $c^*$. This modulation is more or less pronounced depending on the sample. The use of a $2(2)^{1/2}a_c \times 2(2)^{1/2}a_c \times 3a_c$ cell

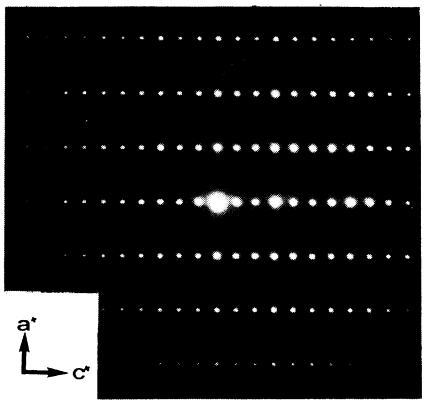


FIG. 1. Electron diffraction pattern along the zone axis [001] of the $Ba_2YCu_3O_7$ sample.

 

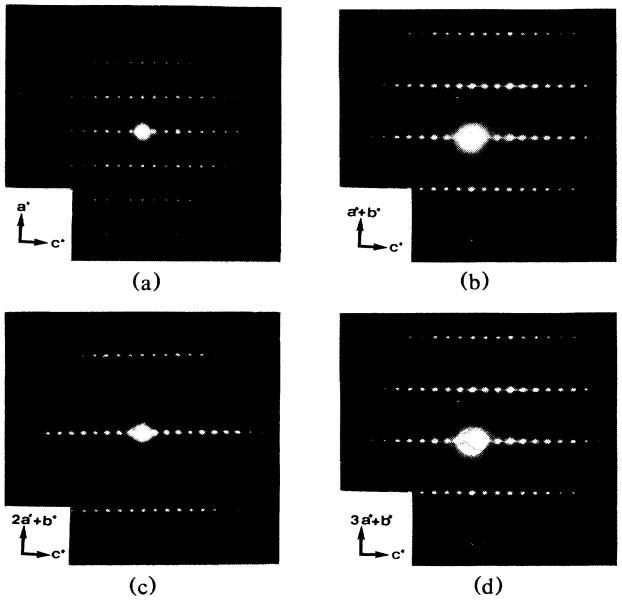


FIG. 2. Electron diffraction patterns along the (a) [0$\bar{1}$0], (b) [1$\bar{1}$0], (c) [1$\bar{2}$0], and (d) [1$\bar{3}$0] zone axis of a reduced sample showing diffuse lines.

(where $a_c$ refers to the pseudocubic perovskite cell) allows us to explain the geometry of the diffuse scattering. This was confirmed by the intersection of these lines with the $a^*b^*$ plane [Fig. 4(b)]. The extinction of the ($h$/4 $k$/4 $l$) diffuse row is not observed in the $a^*b^*$ plane, due to multiple scattering. All crystals which displayed this type of diffuse streaks were confirmed to have tetragonal symmetry.

In the second case, diffuse lines parallel to the $c^*$ axis are present in the electron-diffraction patterns, but they are exclusively located along principal rows, intercepting the (001)* planes at (100), (010), (110),.... The shape of these diffuse streaks is the same as in the first case.

The third type of diffuse scattering, also reported in Ref. 10, is observed in the $a^*b^*$ planes where the streaks are elongated along $a^*$ or $b^*$. The intensities of these streaks are more or less concentrated about the positions ($h$/2 0 0) or (0 $k$/2 0), depending on the crystal studied. In Fig. 3(a), long diffuse streaks link the Bragg reflections. In Fig. 3(b), the diffuse effects are concentrated into elongated spots centered midway between the Bragg spots. Generally, the streaks are directed along both $a^*$ and $b^*$ but their intensity in the two directions can be different. Most of these diffuse streaks are observed on twinned samples having orthorhombic symmetry revealed by the splitting of the Bragg spots. The variation of the intensity of the streaks with the proportion and the orientation of different twinned individuals present in the selected area can be explained by two families of microdomains oriented at 90° to one another. These domains are related to the twinned individuals orientation. If starting with the (001)* plane, a rotation is made around one of the axes, for example $a^*$, towards the planes (0$\bar{1}$1)*, (0$\bar{2}$1)*, etc., the diffuse effects are maintained, centered on positions (0 $\frac{1}{2}$ $l$). This indicates that they are in fact diffuse bands, parallel to $a^*$ (or $b^*$) and $c^*$, with a variable thickness.

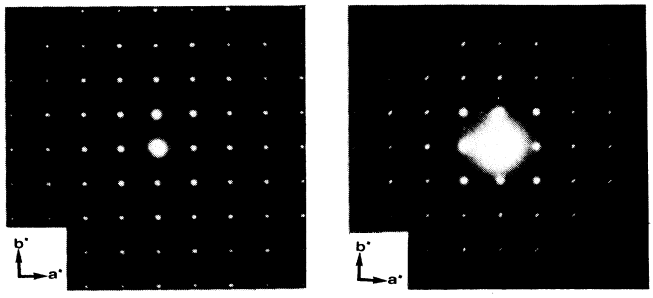


FIG. 3. Electron diffraction pattern of the $a^*b^*$ plane for a reduced sample showing (a) diffuse streaks and (b) the concentration of the diffuse lines into elongated spots.

For the samples of average composition $Ba_2YCu_3O_{6.63}$, $Ba_2YCu_3O_{6.41}$ prepared by slow cooling in argon, and more homogeneous than that quenched in air, the three types of diffuse scattering effects were also observed in general. It is not possible to say, from the samples studied, if one or the other of the three types of diffuse scattering is dominant in $Ba_2YCu_3O_{6.63}$ or in $Ba_2YCu_3O_{6.41}$. For certain samples, however, no diffuse scattering was present. For the sample quenched in liquid nitrogen, and for the sample of composition $Ba_2YCu_3O_{6.10}$, obtained by

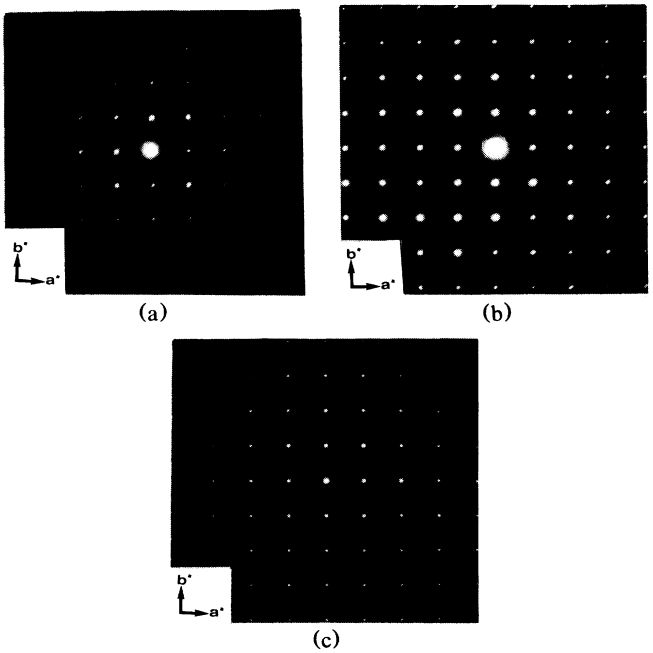


FIG. 4. Electron diffraction pattern along the [001] zone axis of $Ba_2YCu_3O_7$ (a) before, (b) during, and (c) after *in situ* reduction. The short-range ordering, which appears under the beam in the example reported here, corresponds to the first case described (Fig. 2).

slow cooling in argon, no diffuse scattering was observed at all in the electron diffraction pattern.

Starting from a stoichiometric $Ba_2YCu_3O_7$ sample [Fig. 4(a)] presenting no diffuse scattering, it is possible to obtain the diffuse lines or bands by heating the sample with concentration of the electron beam [Fig. 4(b)], then to have them disappear when a higher sample temperature is reached [Fig. 4(c)]. This *in situ* transformation can be associated with an oxygen loss since it does not affect the shape of the Bragg spots and the periodicity of the cell along the $c$ axis. There is only a small change of the cell parameters corresponding to an orthorhombic/tetragonal symmetry transformation. Such a transformation is related to the variation of oxygen composition in Ref. 8. Thus, the lines and bands of diffuse scattering can be attributed to the presence of partially ordered oxygen vacancies. These streaks or bands are always parallel to $c^*$, indicating a lack of long-range order between successive (001) planes. In the first two cases described, the streaks are narrow in the $a^*b^*$ plane, which indicates that the order between the vacancies is well developed in these directions. By contrast, in the third case, the large width of the diffuse bands along $a^*$ indicates a decrease in the correlation length between the vacancies in the direction parallel to $a$.

Because of the variety of the diffuse-scattering effects observed in the different samples, it is difficult to present for each case a simple vacancy ordered model which accounts for the intensities of the streaks or bands. However, the oxygen atoms which are absent in the structure of the reduced phases are those located in the basal plane, at $z=0$ of the orthorhombic cell, given as O(4) in Refs. 3–6. In fact this site is only partially occupied in the phase $Ba_2YCu_3O_{6.8}$ (Ref. 5) and is empty in $Ba_{2.1}Y_{0.9}Cu_3O_6$ (Ref. 7). In addition, the temperature factor of this oxygen is very large in $Ba_2YCu_3O_7$ (Ref. 3). The distance between the (001) planes which contain O(4) is large enough (11.7 Å) to explain the lack of correlation of the oxygen-vacancy ordering along $c$.

We are continuing our structural studies by x-ray, electron, and neutron diffraction on other phases with well-defined oxygen contents. We hope, thus, to be able to relate the various diffuse-scattering effects to specific oxygen contents and to propose models for the ordering of oxygen vacancies.

The Laboratoire de Cristallographie is associé à l'Université Scientifique, Technologique, et Médicale de Grenoble, Centre National de la Recherche Scientifique.

*Permanent address: Faculdade de Ciencias Quimicas, Universidad Complutense, 28040, Madrid, Spain.

†Also at AT&T Bell Laboratories, Murray Hill, NJ 07974.

[1]I. K. Schuller, D. G. Hinks, M. A. Beno, D. W. Capone II, and L. Soderholm, Solid State Commun. (to be published).

[2]J. M. Tarascon, W. R. McKinnon, L. H. Greene, G. W. Hull, and E. M. Vogel, Phys. Rev. B **36**, 226 (1987).

[3]J. J. Capponi, C. Chaillout, A. W. Hewat, P. Lejay, M. Marezio, N. Nguyen, B. Raveau, J. L. Soubeyroux, J. L. Tholence, and R. Tournier, Europhys. Lett. **3**, 1301 (1987).

[4]M. A. Beno, L. Soderholm, D. W. Capone II, D. G. Hinks, J. D. Jorgensen, I. K. Schuller, C. U. Segre, K. Zhang, and J. D. Grace, Appl. Phys. Lett. (to be published).

[5]F. Beech, S. Miraglia, A. Santoro, and R. S. Roth, Phys. Rev. B **35**, 8778 (1987).

[6]W. I. F. David, W. T. A. Harrison, J. M. F. Gunn, O. Moze, A. K. Soper, P. Day, J. D. Jorgensen, M. A. Beno, D. W. Capone II, D. G. Hinks, I. K. Schuller, L. Soderholm, C. U. Segre, K. Zhang, and J. D. Grace, Nature **327**, 310 (1987).

[7]P. Bordet, C. Chaillout, J. J. Capponi, J. Chenavas, and M. Marezio, Nature **327**, 687 (1987).

[8]P. Strobel, J. J. Capponi, C. Chaillout, M. Marezio, and J. L. Tholence, Nature **327**, 306 (1987).

[9]A. W. Hewat, J. J. Capponi, C. Chaillout, and M. Marezio, Nature (to be published).

[10]H. W. Zandbergen, G. Van Tendeloo, T. Okabe, and S. Amelinckx, Phys. Status Solidi (A) (to be published).

[11]B. G. Hyde, J. G. Thompson, R. L. Withers, J. G. Fitzgerald, A. M. Stewart, D. J. M. Bevan, J. S. Anderson, J. Bitmead, and M. S. Paterson, Nature **327**, 402 (1987).

[12]A. Ourmazd, J. A. Rentschler, J. C. H. Spence, M. O'Keeffe, R. J. Graham, D. W. Johnson, Jr., and W. W. Rhodes, Nature **327**, 308 (1987).

[13]M. Hervieu, B. Domenges, C. Michel, and B. Raveau (unpublished).

[14]E. A. Hewat, M. Dupuy, A. Bourret, J. J. Capponi and M. Marezio, Nature (to be published).

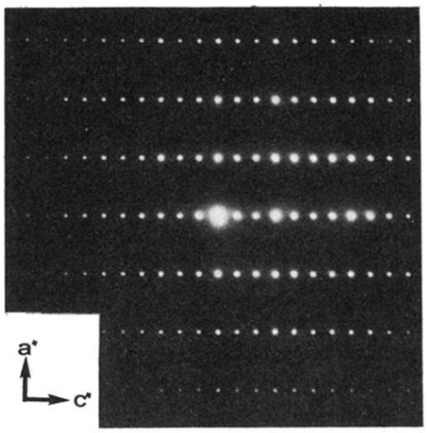


FIG. 1. Electron diffraction pattern along the zone axis [001] of the $Ba_2YCu_3O_7$ sample.

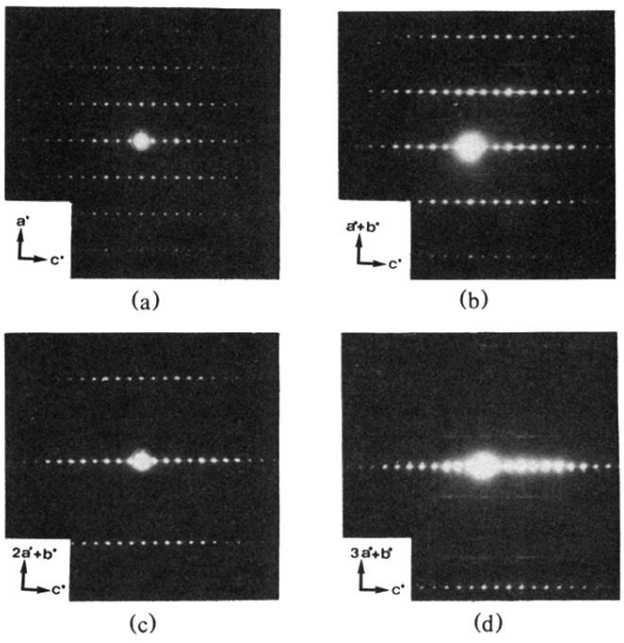


FIG. 2. Electron diffraction patterns along the (a) $[0\bar{1}0]$, (b) $[1\bar{1}0]$, (c) $[1\bar{2}0]$, and (d) $[1\bar{3}0]$ zone axis of a reduced sample showing diffuse lines.

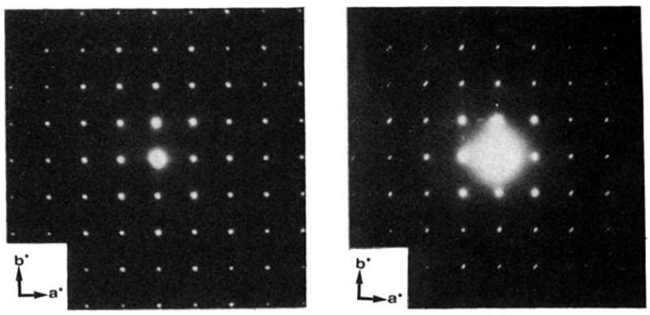


(a) (b)

FIG. 3. Electron diffraction pattern of the $a^*b^*$ plane for a reduced sample showing (a) diffuse streaks and (b) the concentration of the diffuse lines into elongated spots.

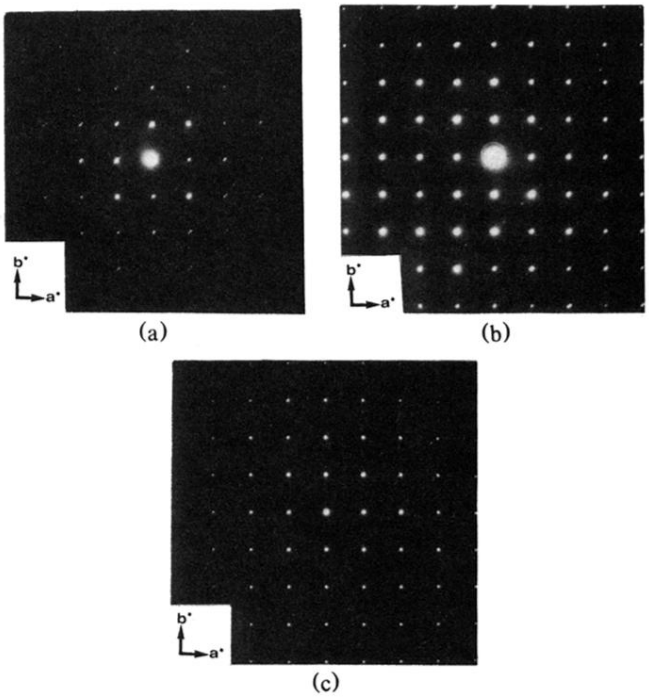


FIG. 4. Electron diffraction pattern along the [001] zone axis of $Ba_2YCu_3O_7$ (a) before, (b) during, and (c) after *in situ* reduction. The short-range ordering, which appears under the beam in the example reported here, corresponds to the first case described (Fig. 2).